Int. J. Heat Mass Transfer. Vol. 33, No. 7, pp. 1545–1562, 1990
Printed in Great Britain

0017–9310/90 $3.00 + 0.00

An observer-based solution of inverse heat conduction problems

WOLFGANG MARQUARDT
Institut für Systemdynamik und Regelungstechnik, Universität Stuttgart, Pfaffenwaldring 9, D-7000 Stuttgart 80, F.R.G.

and

HEIN AURACHER
Institut für Technische Thermodynamik und Thermische Verfahrenstechnik, Universität Stuttgart, Pfaffenwaldring 9, D-7000 Stuttgart 80, F.R.G.

(*Received* 24 *July* 1989)

Abstract—An inverse heat conduction problem arises when temperature measurements are taken in the interior of a body, and the temperature and heat flux on the surface are desired. A new approach to the solution of this class of problems is introduced. It relies on the concept of state and disturbance observers which is well-known from systems theory. The complete temperature profile in the heat conducting body as well as the surface heat flux and temperature can be computed from one or several interior temperature measurements by means of a non-linear distributed parameter observer. The technique is introduced and analysed theoretically by means of a simple tutorial example. The approach is finally applied to a difficult inverse problem of technical significance. The time history of local heat flux and temperature oscillations at the inner surface of an evaporator tube are estimated during transition boiling conditions. Experimental results with boiling refrigerant R114 flowing upward in an electrically heated tube are presented.

1. INTRODUCTION

THE 'inverse problem' of heat conduction constitutes of the determination of surface temperature and heat flux from temperature measurements inside a heat conducting body. In contrast to direct problems, where the solution depends continuously on the initial and boundary conditions, inverse problems are unstable in the sense, that small changes in the data (for example, the measured interior temperatures) can produce large or even unbounded deviations in the solution [1–4]. Therefore, these so-called ill-posed problems are difficult to solve, especially if measurement noise is present.

Inverse problems have been addressed in experimental investigations on heat transfer for a long time. The monograph of Kudryavtsev [5] summarizes the early work of Russian researchers. Various elegant methods based on simplified analytical solutions of the unsteady heat conduction equation are given. They allow an approximate determination of the surface heat flux from temperature measurements inside the body under special, and thus in general restricting, circumstances. Hence, the methods are inapplicable to a wide range of problems, which are characterized, for example, by fast transients or few and noisy measurements. Continuous further development of methods for the solution of inverse heat conduction problems has been in progress in engineering and applied mathematics. They have been discussed in several recent monographs and a large number of contributions in mathematical and engineering journals. Beck *et al.* [1] gave a review with special emphasis on application in heat transfer. In refs. [2–4] fundamental mathematical results on general inverse problems are presented. A number of numerical techniques for problems from various areas of application are compiled in ref. [6]. The solution techniques for inverse problems can be classified in exact methods [1], parameter estimation [1, 6] and regularization techniques [1–4] and difference methods [1, 7]. Most of the recently developed methods tried to minimize the sensitivity of the solution on the specified data (i.e. the measurements) by some mathematical artifice. However, some authors chose a completely different approach. They tried to reformulate the problem in one way or another to avoid, at least to some extent, the ill-posedness of the inverse problem. El Bagdouri and Jarny [8] reformulated the inverse problem as an optimal boundary control problem, which is solved by a standard optimization technique. Despite the promising reformulation, their approach leads to a numerical scheme which is close to a classical zeroth-order regularization technique [1]. Weber [9] replaced the heat conduction equation by an approximate hyperbolic equation. The direct solution of a well-posed initial value problem for the resulting damped wave equation gives good estimates of the unknown quantities at the body's surface.

In the present study, a new approach is chosen to

NOMENCLATURE

a	dimensionless thermal diffusivity, $(\lambda/\rho c_p)(\tau_{ref}/L^2)$
$a^{(i)}$	thermal diffusivity of layer i [$m^2 s^{-1}$]
c_p	specific heat [kJ $kg^{-1} K^{-1}$]
e	dimensionless estimation error (temperature)
$e^{(i)}$	estimation error (temperature) [K]
f_i	control laws [kW m^{-2}]
g	dimensionless heat flux (see equation (2))
h	dimensionless heat flux (see equation (3))
k_i	dimensionless correction factor
k_M	correction factor [s^{-1}]
k_x	correction factor [kW $K^{-1} m^{-2} s^{-1}$]
l_i	boundary of different layers of the composite material [m]
L	length of the one-dimensional heat conduction body [m]
$\dot{m}$	mass flux [kg $m^{-2} s^{-1}$]
p	pressure [bar]
$\dot{q}_x$	heat flux to the fluid [kW m^{-2}]
$\dot{q}_H$	heat flux to the evaporator tube [kW m^{-2}]
r	spatial coordinate [m]
s	eigenvalue
T	temperature [K]
x	dimensionless temperature, $(T-T_{ref})/T_{ref}$
$\dot{x}$	quality [—]
y	dimensionless temperature measurement, $(T_M-T_{ref})/T_{ref}$
z	dimensional spatial coordinate, r/L.

Greek symbols

α_i	Fourier coefficient
γ	abbreviation (see equation (31))
δ	dimensionless error of temperature measurement
ε	dimensionless estimation error (heat flux)
θ	dimensionless thermocouple time constant, ϑ/τ_{ref}
ϑ	thermocouple time constant [s]
λ	thermal conductivity [kW $m^{-1} K^{-1}$]
μ	design deficiency
ξ	dimensionless measurement location, r_M/L
ρ	abbreviation (see equation (39))
ϱ	density [kg m^{-3}]
τ	time [s]
φ_i	dimensionless correction factor
ϕ	correction factor [s^{-1}]
ψ	eigenfunction.

Superscripts

(i)	layer i
$\hat{}$	estimated quantity
$-$	asymptotic state
$\sim$	rough estimate.

Subscripts

i	inner
M	measurement
o	outer
ref	reference
s	setpoint
0	initial condition.

solve inverse heat conduction problems. It is based on the well-known concept of state and disturbance observers, which has been developed in systems theory since the early 1970s for different classes of dynamic systems [10–13]. These methods have been designed to reconstruct the whole system state from a few easily available measurements in real time. The estimated states are used to compute a model-based control law to improve closed-loop control performance of complex systems. Besides the application in control the techniques have also been employed to merely get more quantitative information about a dynamic system from a limited number of measurements. This enhanced process knowledge is a basis for better and more reliable process supervision strategies. Various applications, even on industrial processes, are reported in survey papers [14, 15].

The application of observers to inverse problems results in the solution of an initial value problem for a modified model equation, where the inputs and the system parameters are known. The model outputs which are the unknown quantities of the original inverse problem can be computed in a cause and effect sequence by a common numerical method. Hence, in contrast to most of the other techniques a direct (or forward) problem is solved to compute the interesting quantities such as time histories of surface heat flux and spatial temperature profiles in heat conduction. This direct problem is usually of a better condition than the inverse problem, i.e. it is well posed.

The first part of this paper introduces the observer scheme by means of a simple tutorial inverse heat conduction problem. A theoretical analysis is carried out to give a deeper insight in the strengths and weaknesses of the method. These results are of direct use to design observers for complex inverse heat conduction problems of technical significance. As an example the estimation of surface heat flux time histories in forced convection transition boiling from temperature measurements inside the evaporator wall is presented in the second part. Some experimental results are given to demonstrate the capability of the technique.

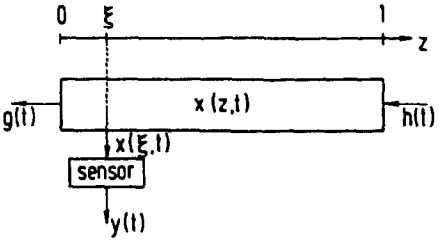

FIG. 1. One-dimensional heat conduction system.

2. A TUTORIAL EXAMPLE

The heat conduction problem (see Fig. 1) to be studied in this section is given by a one-dimensional heat conduction equation in dimensionless form

$$\frac{\partial x}{\partial t}(z,t) = a\frac{\partial^2 x}{\partial z^2}(z,t), \quad z\in(0,1), \quad t>0 \tag{1}$$

with boundary and initial conditions

$$\frac{\partial x}{\partial z}(0,t) = g(t), \quad t\geqslant 0 \tag{2}$$

$$\frac{\partial x}{\partial z}(1,t) = h(t), \quad t\geqslant 0 \tag{3}$$

$$x(z,0) = x_0(z). \tag{4}$$

The heat flux functions $g(t)$, $h(t)$ and the initial temperature profile $x_0(z)$ are assumed to be consistent at $t=0$. In the interior of the body at location $z=\xi$, $0<\xi<1$, a temperature measurement is taken. The measurement device usually does not reveal the exact temperature $x(\xi,t)$. This is a consequence of the unavoidable time lag of the thermocouple sensor and of deterministic or stochastic measurement errors. The measurement model

$$\theta\frac{dy'(t)}{dt} + y'(t) = x(\xi,t), \quad y'(0) = x_0(\xi)$$

$$y(t) = y'(t) + \delta(t).$$

accounts for a sensor time lag of magnitude θ and some unknown additive measurement error $\delta(t)$. A simplification which is adequate to demonstrate the main effects is given as

$$y(t) = x(\xi,t) + \delta(t). \tag{5}$$

This simplified model can be understood to include measurement errors as well as the distortion of the measurement signal due to measurement time lags if the function $\delta(t)$ is chosen suitably.

The inverse problem to be studied is given by equations (1), (3), (5) with known measurement $y(t)$ and heat flux $h(t)$ and unknown initial condition $x_0(z)$ and heat flux $g(t)$. The latter heat flux and the temperature profile $x(z,t)$, especially the surface temperature $x(0,t)$, are supposed to be determined by some mathematical algorithm. A so-called 'observer' will be used for that purpose.

2.1. *The observer equations*

Though the heat conduction problem stated above is linear, the observer design method of Zeitz [12] for non-linear distributed parameter systems is applied. The observer scheme is constructed in complete analogy to linear lumped parameter systems [10, 11]. An important advantage of this approach compared to the observer design method of Köhne [13] for linear distributed parameter systems is its feasibility for more general non-linear heat conduction problems which arise if materials with temperature-dependent physical properties, non-linear heat sources or non-linear boundary conditions due to heat flux control are considered.

For the moment, the heat fluxes at both surfaces $g(t)$, $h(t)$ are assumed to be known quantities. Only the spatial temperature profile (the state) is supposed to be estimated from one temperature measurement. The principal setup of an observer for state estimation by means of the system inputs and measurements is shown in the block diagram of Fig. 2. A mathematical model of the process and of the measurement device is implemented on a computer in parallel to the real process. This model is fed with all known process inputs (here the surface heat fluxes $g(t)$ and $h(t)$). The process output $y(t)$ (here a measured temperature inside the heat conducting body) is compared to the simulated output of the model. Due to unknown initial conditions of the model $x_0(z)$, modelling and measurement errors, the measured and computed (temperature) signal will not coincide. The resulting output error $y(t)-\hat{y}(t)$—a quantitative measure for the estimation quality—is weighted by a correction factor and fed to the process model as an artificial input quantity. The state variables of the model converge to the states of the real process if so-called observability [10–13] is given and if the correction is designed properly. Observability is a structural property of a system requiring all system states to be reflected in the measurements differently. If the dynamics of the observer—a synonym for the process and sensor models corrected by the estimation quality—are chosen to be faster than those of the real process, the observer is able to follow the transients of the real process states in the sense of a servo control system. Hence, after some time the quantity $\hat{x}(z,t)$ can be taken as an estimate of the true process state $x(z,t)$ from the model.

According to Zeitz [12], the observer equations are formed by adding suitable corrections to the model equations (1)–(3). These corrections consist of the weighted estimation quality $y(t)-\hat{y}(t)$. The observer reads as

$$\frac{\partial \hat{x}}{\partial t}(z,t) = a\frac{\partial^2 \hat{x}}{\partial z^2}(z,t) + k_1[y(t)-\hat{y}(t)], \quad z\in(0,1), \quad t>0 \tag{6}$$

$$\frac{\partial \hat{x}}{\partial z}(0,t) = g(t) + k_2[y(t)-\hat{y}(t)], \quad t\geqslant 0 \tag{7}$$

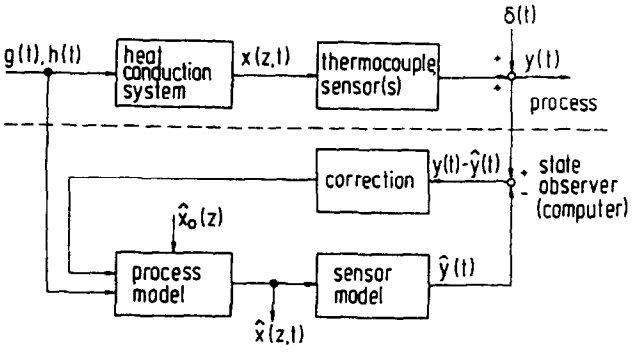

FIG. 2. Block diagram of the state observer scheme.

$$\frac{\partial \hat{x}}{\partial z}(1,t) = h(t) + k_3[y(t) - \hat{y}(t)], \quad t \geqslant 0 \tag{8}$$

$$\hat{x}(z,0) = \hat{x}_0(z) \tag{9}$$

where the estimated measurements are given by the measurement model (5) with zero disturbance

$$\hat{y}(t) = \hat{x}(\xi, t). \tag{10}$$

The correction factors k_i in the observer equations are (non-linear) functions of the state variables and their spatial derivatives as well as of the inputs in general [12]. This basic state observer scheme can be extended if not all inputs are known as it is the case with the heat flux $g(t)$ at the left boundary of the heat conducting body in Fig. 1. Assuming an adequate model for the unknown inputs, which is often termed as a disturbance model, the observer of Fig. 2 is modified. The disturbance model is added and also corrected by the weighted estimation quality (see Fig. 3). If observability is retained the combined state and disturbance observer yields estimates of the process state $\hat{x}(z, t)$ (here the temperature profile) as well as of the input (here the surface heat flux $\hat{g}(t)$) at the same time. This approach which is often used with lumped parameter systems (see, for example, Chap. 3.6 of ref. [16]) is adopted here to estimate one of the boundary conditions of a distributed parameter system.

A simple disturbance model for the unknown heat flux $g(t)$ is given as

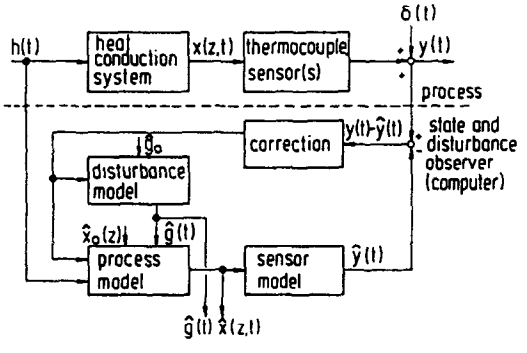

FIG. 3. Block diagram of the state and disturbance observer scheme.

$$\frac{dg(t)}{dt} = 0; \quad g(0) = g_0. \tag{11}$$

A deterministic interpretation of this model reveals a constant heat flux in some small time interval. Models of this type have been successfully employed for disturbance estimation in numerous applications in control.

The equations of the extended observer consist of equations (6)–(9), where the known function $g(t)$ is replaced by the estimated quantity $\hat{g}(t)$. This estimate is determined by the additional observer equation

$$\frac{d\hat{g}(t)}{dt} = k_4[y(t) - \hat{y}(t)], \quad \hat{g}(0) = \hat{g}_0. \tag{12}$$

This equation reveals a fundamental property of observers for the solution of inverse heat conduction problems. The determination of the unknown surface heat flux, which is an input to the model, from the model outputs can be accomplished by an inversion of the model equations. For dynamic problems inversion is performed by one or more differentiations of the outputs with respect to time. Most of the exact analytical formulae for surface heat flux calculations from temperature measurements inside the body depend on differentials of the measurements. As examples the classical methods of Kastelin (p. 36 of ref. [5]) and Burggraf (p. 67 of ref. [1]) or the recent method of Tsoi [17] are referred to, where the temperature measurements must be differentiated infinitely times to determine the surface heat flux. In contrast, in the observer algorithm the surface heat flux is computed by time integration of the measurement. Since integration smoothes high frequency stochastic errors whereas differentiation roughens these signals, the sensitivity of the surface heat flux estimate with respect to measurement noise is lower for observers than for other methods which explicitly or implicitly rely on differentiation(s) of the measurements.

After the observer structure is fixed, the remaining problem is the choice of the functional dependence of the corrections to meet the general requirements on an observer such as asymptotic stability and fast convergence to the states of the real process. This observer

design problem is solved by a study of the appropriate differential equations for the errors between the true and the estimated process states [12]. Introducing the errors

$$e(z,t) = \hat{x}(z,t) - x(z,t)$$
$$\varepsilon(t) = \hat{g}(t) - g(t)$$

the following error equations result after subtraction of the adjacent model and observer equations stated above:

$$\frac{\partial e}{\partial t}(z,t) = a\frac{\partial^2 e}{\partial z^2}(z,t) + k_1[y(t) - \hat{x}(\xi,t)], \quad z \in (0,1), \quad t > 0 \tag{13}$$

$$\frac{\partial e}{\partial z}(0,t) = \varepsilon(t) + k_2[y(t) - \hat{x}(\xi,t)], \quad t \geqslant 0 \tag{14}$$

$$\frac{\partial e}{\partial z}(1,t) = k_3[y(t) - \hat{x}(\xi,t)], \quad t \geqslant 0 \tag{15}$$

$$e(z,0) = e_0(z) \tag{16}$$

$$\frac{d\varepsilon(t)}{dt} = k_4[y(t) - \hat{x}(\xi,t)], \quad \varepsilon(0) = \varepsilon_0. \tag{17}$$

The estimated quantities computed by the observer differ from the true ones by the errors $e(z, t)$ and $\varepsilon(t)$. The design of the observer would be optimal, if

$$e(z,t) \equiv 0, \quad \varepsilon(t) \equiv 0, \quad \forall z, t \tag{18}$$

could be accomplished. This is not possible in general because of non-zero initial conditions $e_0(z)$ and ε_0. If the corrections could be chosen according to

$$k_1[y(t) - \hat{x}(\xi,t)] = -\varphi_1 e(z,t) \tag{19}$$
$$\varepsilon(t) + k_2[y(t) - \hat{x}(\xi,t)] = 0 \tag{20}$$
$$k_3[y(t) - \hat{x}(\xi,t)] = 0 \tag{21}$$
$$k_4[y(t) - \hat{x}(\xi,t)] = -\varphi_2 \varepsilon(t) \tag{22}$$

the errors would be determined by a set of homogeneous equations with sink terms of strengths φ_1, φ_2. For arbitrary initial conditions their solutions tend to zero for increasing t. Hence, criteria (18) can be approximated arbitrarily close

$$|e(z,t)| \leqslant eps, \quad |\varepsilon(t)| \leqslant eps, \quad \forall z, t \geqslant t^*. \tag{23}$$

The rate of convergence, represented by the values of *eps* and t^*, can be determined by a proper choice of the (positive) design parameters φ_1, φ_2. The implementation of the correction terms as stated in equations (19)–(22) requires an exact knowledge of the errors $e(z, t)$ and $\varepsilon(t)$ which is obviously not available. To resolve this difficulty the design methodology is approximated by the following choice of the weights in the error equations (13)–(17):

$$k_2 = k_3 = 0, \qquad k_4 = -k, \quad k > 0$$
$$k_1[y(t) - \hat{x}(\xi,t)] = -\varphi[\hat{x}(z,t) - \tilde{x}(z,t)], \quad \varphi > 0.$$

The quantity $\tilde{x}(z, t)$ is a rough estimate of the true spatial profile $x(z, t)$, which is adequate to determine the correction term. This rough estimate could be computed for example by the simple linear trial function $\tilde{x}(z, t) = c_1(t)z + c_2(t)$, where the coefficients are determined from the known functions $h(t)$ and $y(t)$. Using

$$\mu(z,t) = x(z,t) - \tilde{x}(z,t) \tag{24}$$

as an abbreviation, the final error equations read as follows:

$$\frac{\partial e}{\partial t}(z,t) = a\frac{\partial^2 e}{\partial z^2}(z,t) - \varphi[e(z,t) - \mu(z,t)], \quad z \in (0,1), \quad t > 0 \tag{25}$$

$$\frac{\partial e}{\partial z}(0,t) = \varepsilon(t), \quad t \geqslant 0 \tag{26}$$

$$\frac{\partial e}{\partial z}(1,t) = 0, \quad t \geqslant 0 \tag{27}$$

$$e(z,0) = e_0(z) \tag{28}$$

$$\frac{d\varepsilon(t)}{dt} = -k[\delta(t) - e(\xi,t)], \quad \varepsilon(0) = \varepsilon_0. \tag{29}$$

The estimation quality of the observer with respect to criteria (23) is discussed in the next section by a theoretical analysis of the error equations.

2.2. *Analysis of the error equations*

Since the error equations (25)–(29) are linear, a closed solution could be deduced. This solution, however, is too complex to assess qualitative features of the solutions $e(z, t)$ and $\varepsilon(t)$.

Instead of an analytical solution we first look at the eigenvalues of the set of equations (25)–(29), which display the qualitative dynamic behaviour such as stability and rate of convergence to an asymptote for large times. Due to the time varying forcing functions $\mu(z, t)$ and $\delta(t)$ this asymptote is not a steady state in general. As shown in Appendix A, the eigenvalues s are determined by the transcendent characteristic equation

$$0 = \gamma s \sinh \gamma + k \cosh \gamma(1 - \xi) \tag{30}$$

$$\gamma = \sqrt{\left(\frac{\varphi + s}{a}\right)}. \tag{31}$$

This equation has an infinite number of complex solutions s_i. For two limiting cases of the g-correction k, the eigenvalues can be determined explicitly to be

$$s_{-1} = 0 \quad \text{and} \quad s_i = -a(i\pi)^2 - \varphi, \quad i = 0, 1, 2, \ldots \quad \text{for} \quad k \to 0 \tag{32}$$

$$s_i = -\frac{a\pi^2}{(1-\xi)^2}\left(\frac{2i+1}{2}\right)^2 - \varphi, \quad i = 0, 1, 2, \ldots \quad \text{for} \quad k \to \infty. \tag{33}$$

Since all eigenvalues are real and not positive, the

observer scheme is always stable in the limiting cases. For $k = 0$, no satisfactory estimate can be accomplished because of the zero eigenvalue in the spectrum (32); an error in the boundary condition $\varepsilon(t)$ would stay at its initial value ε_0 at time $t = 0$ (see equation (29)). Numerical solutions of equation (30) have shown that for intermediate values of k instabilities may arise. They are indicated by some eigenvalues with positive real part. A necessary condition for the choice of the tuning parameters is a stable observer or in other words eigenvalues with negative real parts. This condition can be checked directly by a numerical solution of the characteristic equation (30) or by dynamic simulation of the observer equations (6)–(9) and (12).

The rate of convergence of the errors to zero is determined by the magnitude of the real part of the eigenvalues. The estimation errors decay faster the smaller all the (negative) real parts of the eigenvalues are. The characteristic equation and the eigenvalues in the limiting cases reveal that the rate of convergence is influenced by the type of material (a), the location of the sensor (ξ) and both tuning parameters (k, φ). The quantities a and ξ are usually fixed by the experimental setup under consideration. The rate of convergence can be manipulated by proper choice of k and φ. For large values of k it is determined mainly by the magnitude of φ (see equation (33)).

Another question of practical importance is the magnitude of the asymptotic estimation errors for large times. They are not equal to zero, since there are non-zero driving functions $\mu(z, t)$ and $\delta(t)$ in the error equations (25)–(28). To facilitate the analysis we assume that the dynamics of the homogeneous error equations are much faster than typical variations of the forcing functions with time. This assumption is always valid for fast observers, i.e. for large tuning parameters k and φ. Then, the errors follow the forcing functions in a quasi-steady manner and are given by

$$0 = a\frac{\partial^2 \bar{e}}{\partial z^2}(z, t) - \varphi[\bar{e}(z, t) - \mu(z, t)], \quad z \in (0, 1) \tag{34}$$

$$\frac{\partial \bar{e}}{\partial z}(0, t) = \bar{\varepsilon}(t) \tag{35}$$

$$\frac{\partial \bar{e}}{\partial z}(1, t) = 0 \tag{36}$$

$$\bar{e}(\xi, t) = \delta(t) \tag{37}$$

where $\bar{e}(z, t)$ and $\bar{\varepsilon}(t)$ are defined as

$$\lim_{t \to \infty} e(z, t) = \bar{e}(z, t), \quad \lim_{t \to \infty} \varepsilon(t) = \bar{\varepsilon}(t).$$

The solution $\bar{e}(z, t)$ of the boundary value problem (34)–(36) with time t as a parameter is accomplished by Green's function method [18]. The unknown asymptotic error in the heat flux at the left boundary $\bar{\varepsilon}(t)$ can be calculated from equation (37) to be

$$\bar{\varepsilon}(t) = \rho^2 \int_0^{\xi} \mu(\zeta, t) \cosh \rho\zeta \, d\zeta + \frac{1}{\cosh \rho(1-\xi)} \left\{ \rho^2 \cosh \rho\xi \int_{\xi}^{1} \mu(\zeta, t) \cosh \rho(1-\zeta) \, d\zeta - \rho \sinh \rho \, \delta(t) \right\} \tag{38}$$

where

$$\rho = \sqrt{\left(\frac{\varphi}{a}\right)}. \tag{39}$$

It should be noted here that the asymptotic error is completely independent of the tuning parameter k. Hence, k is only responsible for the rate of convergence. One should not conclude to choose φ as small and k as large as possible. For small ω the assumption which leads to equation (38) is not valid any more. The estimation of the surface heat flux would not be of sufficient quality in this case. The magnitude of the design parameter k (and φ) is limited above if significant measurement noise is present. For linear lumped parameter systems a detailed analysis of the relationship between the magnitude of the observer correction and the amplification of measurement noise in the estimates reveals that the dynamic behaviour of infinitely fast observers—being characterized by infinitely large corrections—imposes high-order differentiations on the measurements [19, 20]. Hence, for increasing corrections the smoothing property referred to above gradually ceases to be valid.

The discussion of relation (38) with respect to some limiting cases in Appendix B and our knowledge of the eigenvalues of the observer for large k allow us to state some guide lines to avoid significant asymptotic errors in the heat flux estimates and to enhance the rate of convergence.

- Large values of ρ improve convergence. However, the influence of measurement errors $\delta(t)$ and design deficiencies $\mu(z, t)$ tends to be smaller the lower the magnitude of ρ is. The rate of convergence should therefore be improved by enlarging the value of k alone and not that of φ. However, k (and φ) must be limited above to avoid significant amplification of measurement errors in the estimates.
- The estimation is facilitated with small values of ξ, i.e. with a measurement close to the surface under consideration. For large values of ρ and good measurements (small $\delta(t)$) the influence of the design deficiency $\mu(z, t)$ almost vanishes; very good estimates are accomplished in this case.
- Significant measurement errors lead to large estimation errors if the measurement is located deep in the heat conducting body.
- The design deficiency $\mu(z, t)$ should vanish in the spatial mean for each time. This can be accomplished approximately by proper choice of $\tilde{x}(z, t)$.

The developed guide lines are of direct use for the design of observers to solve inverse heat conduction problems. They are also valid at least approximately for more complex problems as experience has shown.

2.3. *Implementation, tuning and evaluation of the observer*

The algorithmic implementation of the observer is a standard problem. In general, only a numerical solution of the coupled partial and ordinary differential equations is tractable. A method of lines approach is best suited for that purpose. The spatial differential operator in the observer equations is discretized by some approximation scheme like finite differences, finite elements or a Galerkin method, finally leading to a system of ordinary differential equations in time [21]. These equations are combined with the measurement model and solved simultaneously with some standard integration algorithm for systems of stiff ordinary differential equations [22]. The accuracy of the solution is determined by the quality of the spatial approximation and by the error of the time integration. The number of grid nodes, which is required to achieve a certain degree of approximation, can be determined a priori by numerical solution of the direct problem such that the difference to a solution with more nodes is negligibly small. Discretization errors of the time integration are controlled by adjusting the integration time step automatically to meet user specified error tolerances. Sufficient accuracy of the numerical results can be guaranteed independently from the observer design parameters. This is not true with difference methods for inverse heat transfer problems, where the discretization parameters usually coincide with the tuning parameters of the algorithm [1].

The first step of observer tuning and evaluation is carried out by simulation. For that purpose, the process and the observer are implemented in the simulator according to the block diagram of Fig. 3. The unknown heat flux function $g(t)$ is assumed in the simulation to test the estimation scheme. The simulation of the heat conduction system yields the time history $y(t)$ which is supplied by the thermocouple in real experiments. The simulated measurement is fed to the observer. To generate 'real' experimental measurements random noise can be added according to equation (5). The estimated temperature profile $\hat{x}(z, t)$ and surface heat flux $\hat{g}(t)$ can be compared to the 'true' values of the simulated process. Thus, the estimation quality can be judged easily. By proper selection of test signals $g(t)$ the observer can be optimized by the choice of the tuning parameters according to the requirements of the peculiar estimation problem under consideration. An example for the design procedure will be given with the technical problem of the next section.

After the observer scheme is optimized in simulations, the simulated measurements are replaced by temperature readings from the real experiment and are fed to the observer after A/D conversion. Since the observer uses only past but no future information the processing of the measurement can be carried out on-line if sufficient computing power is available to solve the observer equations in real-time.

3. AN INVERSE PROBLEM FROM TRANSITION BOILING

The inverse heat conduction problem to be solved by the observer technique introduced in the last section arises from the experimental study of the largely unknown wetting characteristics and heat transfer laws in forced convection transition boiling [23]. The heat transfer experiments are carried out with refrigerant R114 as a test fluid by means of a closed experimental test loop with a vertical tube as test section. The main evaporator consists of a cylindrical copper block of 32.7 mm o.d. soldered onto a nickel tube with 1 mm wall thickness and 14 mm i.d. The copper block is heated by a sheathed resistance wire, rolled and brazed into a coiled channel on the copper surface. The evaporator is equipped with a couple of radially mounted thermocouples to detect the wall temperature. Steady-state experiments are carried out in the transition boiling region. Hence, feedback control of the wall temperature is required. One of the thermocouples serves as a sensor to give the setpoint deviation of the wall temperature for the control system used. A detailed description of the experimental setup and of the control system is presented in refs. [23, 24].

The local temperature and heat flux variations at the inner surface of the main evaporator can be employed for monitoring the wetting characteristics of the boiling fluid. This information is essential for a profound understanding of the boiling mechanism. Since the surface temperature cannot be measured directly without disturbing the boiling phenomena, an inverse problem must be solved to compute the time varying local surface temperature and the local heat flux from the heater wall to the evaporating fluid from temperature measurements below the heating surface. Due to the high frequency of the fluctuations in the unknown quantities, this inverse heat conduction problem is rather difficult to solve by any technique [1].

An angular cross-section of the evaporator tube is shown in Fig. 4. It consists of three layers: the inner nickel tube, the solder and the outer copper block. The thermocouple, which will be used for wetting analysis and control of unstable boiling experiments, is soldered below the surface of the nickel tube at radial position r_M. The electric heater supplies the heat flux $\dot{q}_H(\tau)$ to the evaporator. The heat flux $\dot{q}_x(\tau)$ denotes the heat flux from the evaporator wall to the evaporating fluid. Due to the wetting fluctuations on the inner tube wall, all the heat fluxes and temperatures must be considered as functions of time even in the case of steady-state experiments. Though the

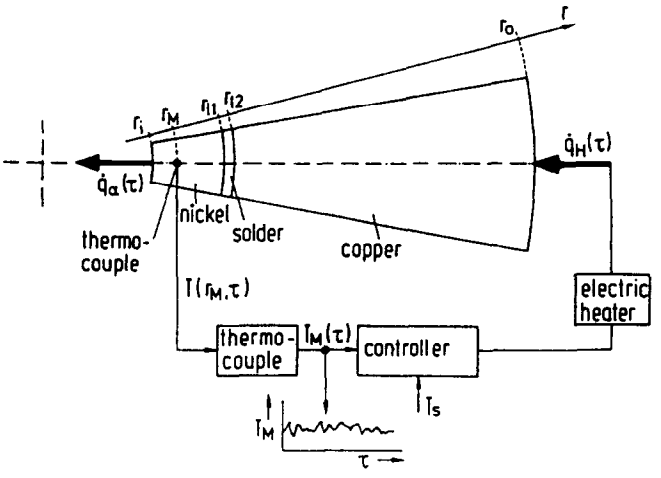

FIG. 4. Schematic of the experimental setup; cross section of the evaporator tube with associated measurement and control system.

time averages of both heat flows are equal, the fluctuations around these mean values will differ as a consequence of the heat capacity of the wall. The flux $\dot{q}_H(\tau)$ is known at any time, since it can be calculated from the measured temperature $T_M(\tau)$ by means of a mathematical model of the heater and the controller. This is not true for $\dot{q}_z(\tau)$ which is determined by the stochastic wetting at the inner tube wall.

3.1. *Observer design*

The dynamic behaviour of the evaporator wall is assumed to be modelled adequately by a one-dimensional heat conduction equation in the radial direction for a composite material. The temperature gradients at the inner and outer tube wall

$$\lambda^{(1)}\frac{\partial T^{(1)}}{\partial r}(r_i,\tau)=\dot{q}_z(\tau) \tag{40}$$

$$\lambda^{(3)}\frac{\partial T^{(3)}}{\partial r}(r_o,\tau)=\dot{q}_H(\tau) \tag{41}$$

are determined by the surface heat fluxes $\dot{q}_z$ and $\dot{q}_H$. The upper indices refer to the different materials (see Fig. 4) nickel (1) (solder (2)) and copper (3). The heat flux $\dot{q}_H$ is related to the measured temperature $T_M(\tau)$ and to some controller setpoint T_s by the non-linear control law

$$\dot{q}_H(\tau)=f_1[T_M(\tau)]+f_2(T_s). \tag{42}$$

The control of the evaporator which is open-loop unstable during transition boiling conditions is discussed in detail in ref. [24]. The thermocouple model

$$\vartheta\frac{dT_M(\tau)}{d\tau}+T_M(\tau)=T^{(1)}(r_M,\tau),\quad T_M(0)=T_{M_0} \tag{43}$$

a first-order lag with time constant ϑ relates the indicated temperature at the thermocouple to the true temperature in the heat conducting body.

The unknown heat flux $\dot{q}_z(\tau)$ is represented by a simple model of type (11)

$$\frac{d\dot{q}_z(\tau)}{dt}=0,\quad \dot{q}_z(0)=\dot{q}_{z_0}. \tag{44}$$

This model must be used, since the true heat transfer process is too complex to be modelled with some detail. Nevertheless, it will be shown that the observer calculation yields reliable estimates for the true $\dot{q}_z$.

The observer equations for the evaporator tube are formed in complete analogy to the tutorial example of the previous section

$$\frac{\partial\hat{T}^{(i)}}{\partial\tau}(r,\tau)=a^{(i)}\left(\frac{1}{r}\frac{\partial\hat{T}^{(i)}}{\partial r}(r,\tau)+\frac{\partial^2\hat{T}^{(i)}}{\partial r^2}(r,\tau)\right)-\phi\tilde{e}^{(i)}(r,\tau),\quad i=1(1)3 \tag{45}$$

$$\lambda^{(1)}\frac{\partial\hat{T}^{(1)}}{\partial r}(r_i,\tau)=\hat{\dot{q}}_z(\tau) \tag{46}$$

$$\lambda^{(1)}\frac{\partial\hat{T}^{(1)}}{\partial r}(r_{l_1},\tau)=\lambda^{(2)}\frac{\partial\hat{T}^{(2)}}{\partial r}(r_{l_1},\tau) \tag{47}$$

$$\lambda^{(2)}\frac{\partial\hat{T}^{(2)}}{\partial r}(r_{l_2},\tau)=\lambda^{(3)}\frac{\partial\hat{T}^{(3)}}{\partial r}(r_{l_2},\tau) \tag{48}$$

$$\lambda^{(3)}\frac{\partial\hat{T}^{(3)}}{\partial r}(r_o,\tau)=f_1[T_M(\tau)]+f_2(T_s) \tag{49}$$

$$\hat{T}^{(i)}(r,0)=\hat{T}_0^{(i)}(r),\quad i=1(1)3. \tag{50}$$

$$\frac{d\hat{T}_M(\tau)}{d\tau}=\frac{1}{\vartheta}[\hat{T}^{(1)}(r_M,\tau)-\hat{T}_M(\tau)]+k_M[T_M(\tau)-\hat{T}_M(\tau)],\quad \hat{T}_M(0)=\hat{T}_{M_0}. \tag{51}$$

$$\frac{d\hat{\dot{q}}_z(\tau)}{d\tau}=k_z[T_M(\tau)-\hat{T}_M(\tau)],\quad \hat{\dot{q}}_z(0)=\hat{\dot{q}}_{z_0}. \tag{52}$$

A rough estimate of the time-dependent spatial profiles of the temperature error $e^{(i)}(r, \tau)$ in each layer i of the tube is accomplished by means of a spatial function of exponential type which coincides at position $r = r_M$ with the known output error. The remaining parameters of the observer are ϕ, k_M and k_z. They must be tuned in simulation experiments using the guide lines as developed above. The unknown initial conditions for the observer equations are determined from the assumption of zero fluctuations of $\dot{q}_z$ in a steady-state experiment. More details on the determination of the model parameters (especially the thermocouple time constant ϑ) and on the design of the observer structure by analysis of the adjacent error equations may be found in ref. [25].

The observer (and the process model during observer tuning) is implemented by means of a general purpose software package for the transient simulation of chemical engineering processes [26], which also supports the design and the evaluation of observers [27]. The package is block-oriented in the sense that complex simulation problems can be defined on the basis of standardized model blocks for different equipment stored in a model library.

A rectangular wave with non-zero mean is chosen as a test function $\dot{q}_z(\tau)$ for observer tuning. Three representative test frequencies of 5, 16 and 25 Hz have been determined by a Fourier analysis of measured temperature fluctuations and the following considerations. Low frequency fluctuations which form the main contribution to the temperature signal under transition boiling conditions [23] must be matched very closely. Temperature signal components occurring in a medium frequency range (10–20 Hz) must be matched satisfactorily, whereas fluctuations of significant amplitude well above 20 Hz are rather a result of the signal processing than of the wetting of the heat transfer surface due to the thermal inertia of the system and the damping of the thermocouple. To prevent misinterpretation of the experimental results, signal components in the higher frequency range should be damped in amplitude by the observer algorithm itself in addition to a possible low pass filtering of the measured temperatures (see Section 3.2). Figure 5 shows the simulation results for the final set of tuning parameters with the three test signals. A tradeoff between estimation quality and sensitivity to measurement noise has been established. Higher corrections (k, φ) would result in a significant amplification of measurement noise.

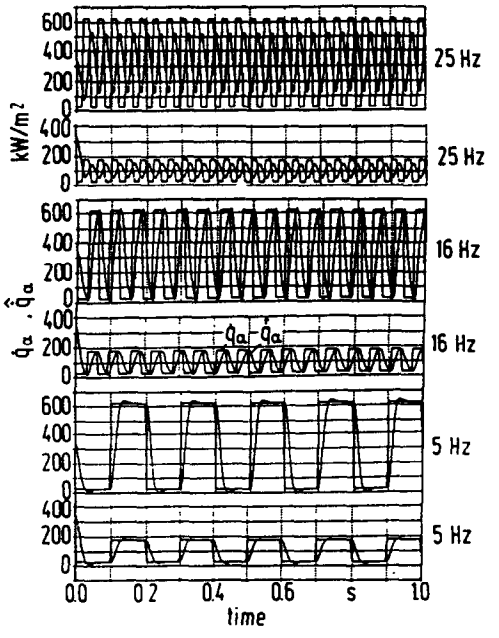

FIG. 5. Evaluation of the observer design for different rectangular heat flux oscillations. $\phi = 1.6 \times 10^3\ s^{-1}$, $k_M = 2 \times 10^3\ s^{-1}$, $k_z = 4 \times 10^6\ kW\ K^{-1}\ m^{-2}\ s^{-1}$.

3.2. *Experimental results*

Since real-time estimation is not required in this application, the analogue temperature measurements taken from the experiments under different boiling conditions are digitized and recorded by means of a transient recorder. The digital measurement signal is transferred to the computer for processing by the observer algorithm. The estimated temperature profile $\hat{T}(r, \tau)$ and the surface heat flux $\hat{\dot{q}}_z(\tau)$ are a result of the computations.

Preliminary simulation experiments have shown that high frequency noise may result in significant errors in the heat flux estimates. A Fourier analysis of experimental temperature data reveals some measurement noise at frequencies well above 20 Hz. A low pass filter is therefore used in the experiments to eliminate high frequencies which from physical reasons must result from noise. An important question is the choice of an optimal corner frequency of the signal filter above which the noise and possibly part of the wanted signal is damped significantly. Due to the heat capacity of the evaporator tube between the measurement location and the inner surface high frequency oscillations in $\dot{q}_z$ are damped to amplitudes of the size of the experimental uncertainties. Heat flux fluctuations of a frequency of 20 Hz and of a typical mean amplitude lead to temperature oscillation amplitudes at the thermocouple position of about 0.05 K. This is comparable to the uncertainty resulting from the thermocouple position and time constant [23, 25]. Such fluctuations are further damped by the thermocouple itself, which reveals a corner frequency of about 2.7 Hz. A low pass filter with a significantly higher corner frequency of 16 Hz is chosen to smooth measured temperatures before A/D conversion and processing by the observer algorithm. Hence, high frequency measurement noise is eliminated. The filter, however, also modifies the wanted signal—especially in the range of the corner frequency—to some extent. Its use should therefore be renounced. In our application the filter is indispensable, since the high frequency noise superimposing our measurements would

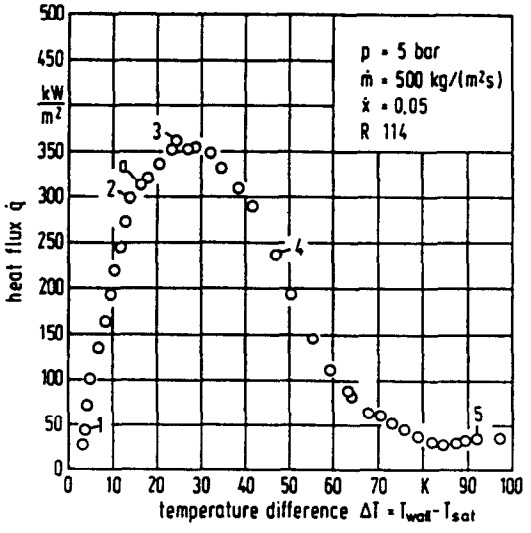

FIG. 6. Boiling curve of refrigerant R114.

lead to gross estimation errors in the estimated heat flux amplitude as simulations with noisy measurements have shown.

Temperature fluctuations are analysed for a complete boiling curve shown in Fig. 6. In Fig. 7 five typical results for different boiling regions are presented. The respective data are marked in Fig. 6. Each plot in Fig. 7 shows the thermocouple reading $T_M(\tau)$, the estimated surface temperature $\hat{T}(r_1, \tau)$ and heat flux $\hat{q}_x$. The plots clearly indicate, that the difference between the measured and the surface temperature, $T_M(\tau) - \hat{T}(r_1, \tau)$, is proportional to the surface heat flux $\hat{q}_x$ plotted in the upper part of the diagrams. The slope of the boiling curve (Fig. 6) beyond the critical heat flux starts to decrease remarkably at state No. 2. This is the region where the temperature amplitudes begin to increase continuously until state No. 4 is reached. Then, they decrease again to the level shown in plot No. 5, which represents the film boiling region. It is in state No. 2 where the heat transfer coefficient reaches its maximum [23]. It seems that this region marks the end of pure nucleate boiling. We assume that at higher wall temperatures already small vapour spots are generated on the wall. They lead to higher amplitudes and a signal characteristic with an increasing contribution of low frequencies in the temperature estimates. The computed surface temperature fluctuations in nucleate boiling (state No. 1) can hardly be the result of pure nucleation. The presumable bubble frequency is significantly higher than the frequency of the fundamental wave (15–20 Hz) of the temperature fluctuations. High frequency signal components which result from nucleation of single bubbles reveal very small amplitudes. They could hardly be detected by the thermocouple sensor if the thermal inertia of the system and the low pass filtering are taken into account. Further, it can be shown experimentally by a study of displayed temperature readings in convective heat transfer that the band width of the superimposing noise is significantly smaller (about 30%) than the one in state No. 1 of Fig. 7. Therefore, the fluctuations of state No. 1 are most likely a result of vapour generation at the heated surface. The phenomenon could be explained by an interference of a few bubbles generated in the vicinity of the thermocouple dip with slightly differing frequencies. Another interesting fact is the negative heat fluxes occurring in the film boiling region (signal No. 5) during very short periods of time. It could probably result from hot vapour spots contacting the surface immediately after a local temperature decrease. Such questions will be the subject of further investigations.

In the literature, it is often assumed that transition boiling is characterized by a combination of film boiling and nucleate boiling each of which alternately occurs on the heating surface. The dependence of the average heat transfer rate on the temperature difference is considered to be primarily a result of the variations in the time fraction, for which nucleate or film boiling conditions exist at a given location. Our results indicate that the real situation is more complex. In Fig. 8 the amplitude variations of surface heat flux and temperature determined by the observer are presented for different data points along the boiling curve. Even if we take into account the possible error of such amplitudes (see Section 3.3), it is quite clear that the concept of an oscillation of the heat flux between more or less constant limiting values is far from the physical reality. Future studies are required to develop a more realistic model of the transition boiling mechanism.

3.3. *Reliability of the estimation results*

The proper interpretation of the experimental results requires a detailed analysis of the reliability of the estimation. Some aspects concerning the estimation quality, such as representation of amplitude, phase and shape of the test signal, are discussed first by means of the simulations in Section 3.1. Figure 5 shows that in case of 5 Hz oscillations, amplitude and even wave form is matched satisfactorily. The observer is able to follow heat flux fluctuations up to 16 Hz, where the amplitude is estimated adequately but the wave form cannot be reproduced properly. The amplitudes of the 25 Hz test signal are damped significantly in the estimation. As referred to above, the damping of high frequency signal components is considered as a welcome effect, since it prevents misinterpretation of noise as a boiling phenomenon. In all cases a phase lag is apparent and the signal shape is not matched exactly. Due to the servo control property of the observer these deficiencies are unavoidable in principle. They could be diminished only if larger corrections are employed at the expense of a higher sensitivity to noise. The phase lag is without significance in our application since only information on the heat flux oscillation amplitudes is of interest for an interpretation of the boiling phenomena. The same is true for the signal shape as long as the fluctuation amplitudes are estimated properly. If

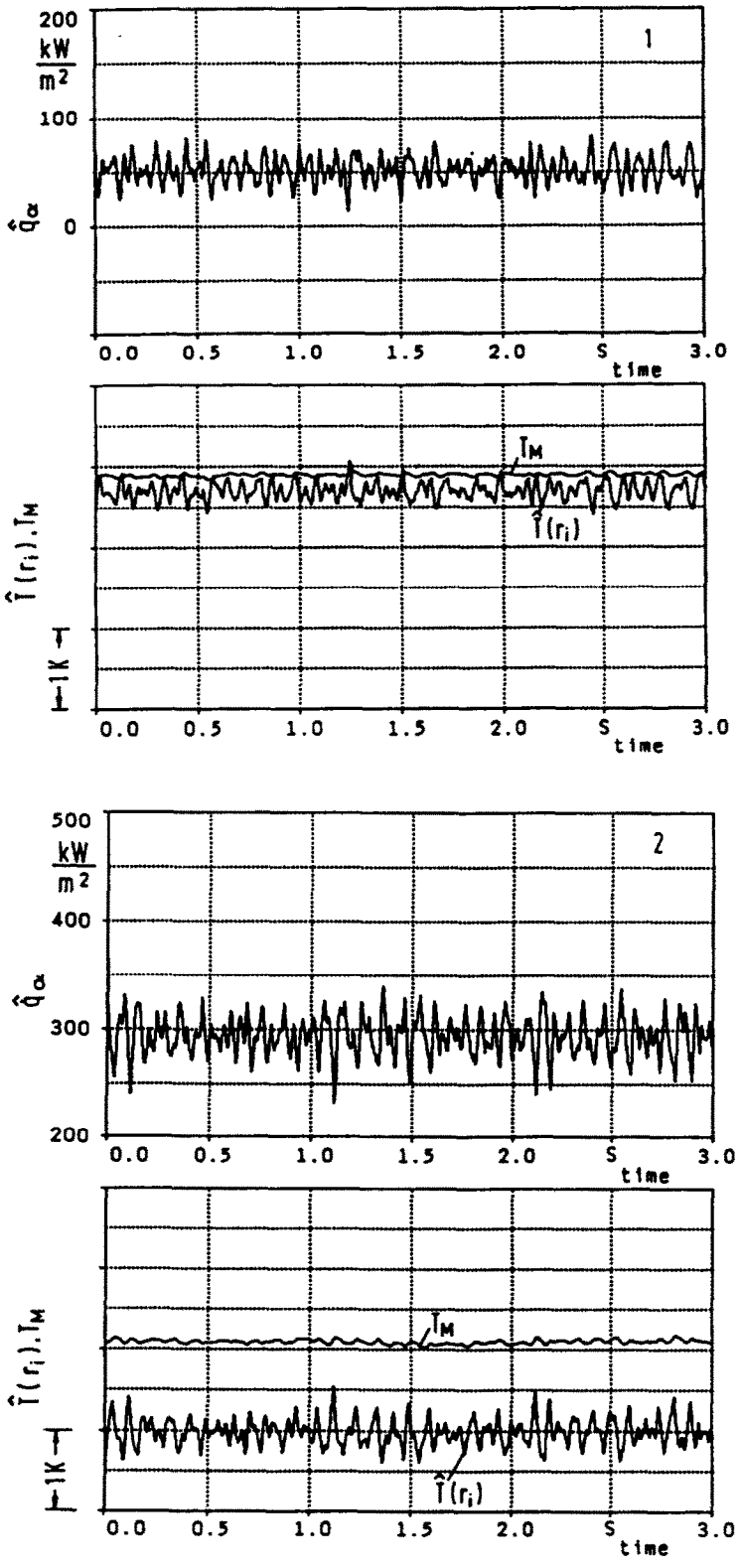

FIG. 7. (1–5) Computed surface heat flux $\dot{q}_z(\tau)$ and temperature $T(r_i, \tau)$ in different boiling regions (see Fig. 6).

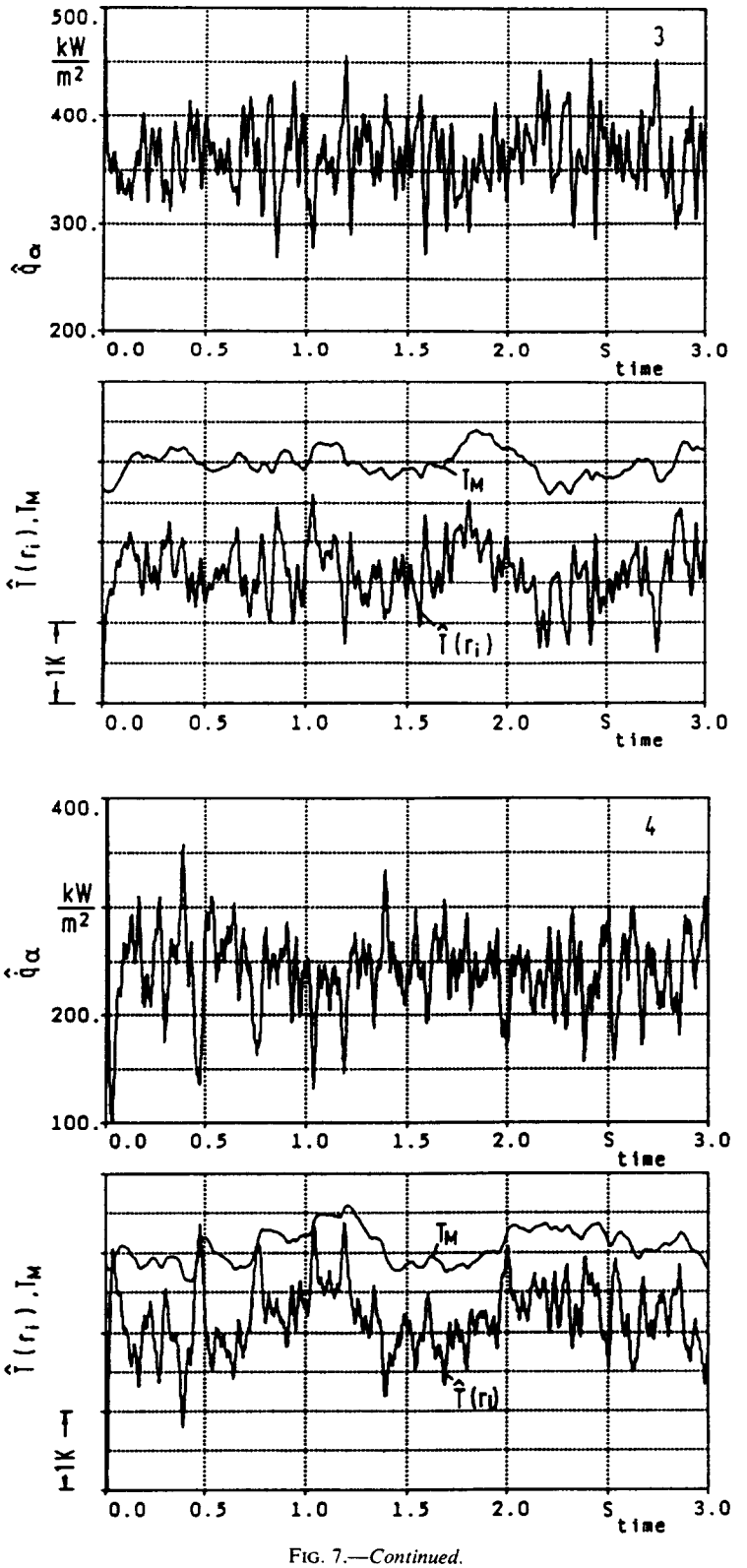

FIG. 7.—*Continued.*

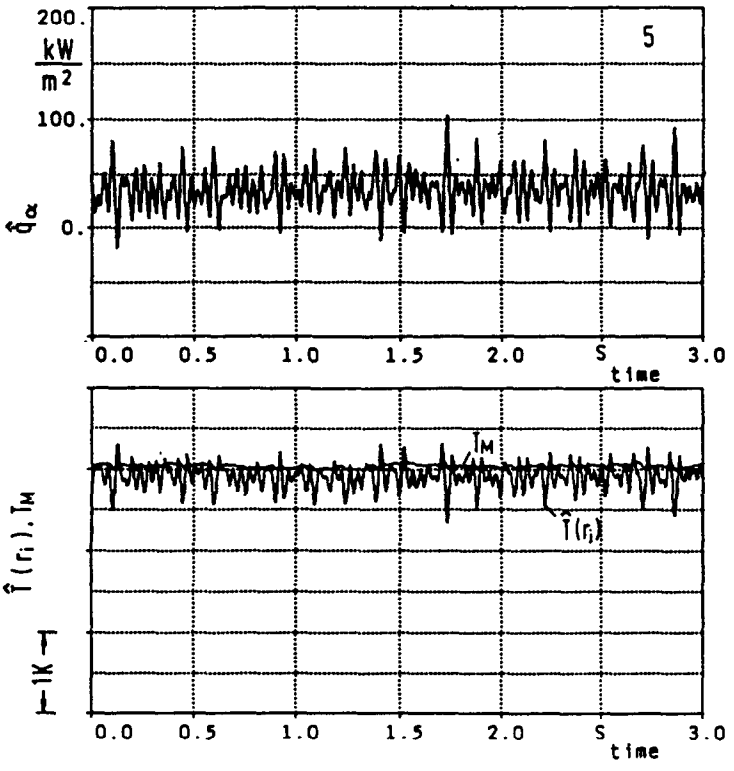

FIG. 7.—*Continued.*

an exact process model and temperature measurements with negligible noise are assumed as it has been the case in the examples of Fig. 5, the estimated fluctuation amplitudes above 16 Hz are too small. The magnitude of the amplitude error increases with increasing frequencies of the heat flux fluctuations.

As for any solution technique of inverse heat conduction problems the most serious errors are a consequence of imperfect modelling. Possible sources of significant errors are the system parameters and the structure of the disturbance (heat flux) and the process (evaporator) model.

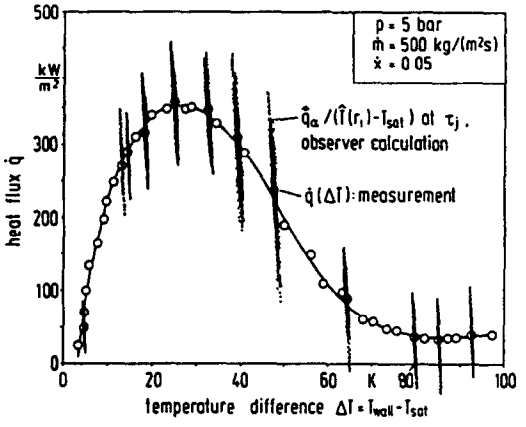

FIG. 8. Heat flux/temperature variations at the surface along the boiling curve; each point in the plotted amplitude bands represents a computed data set $(\hat{q}_\alpha, \hat{T}(r_i) - T_{sat})$ at a given time τ_j; the circles represent the time and space averaged values $(\dot{q}, \Delta T)$.

The most uncertain parameters are time constant and radial position of the thermocouple. A detailed analysis [23, 25] shows that the relative errors in the temperature signals are well below 0.1 K. A variation of the thermocouple time constant and radial position, of the controller gain and of the thermal conductivities has been carried out. Some results are shown in Figs. 9–11. The frequency and amplitude characteristics of the fluctuations are retained in all cases. The errors in the heat flux amplitudes are negligible for an erroneous control gain. Figures 9 and 10 compare the estimation results computed with the nominal value of the position r_M and time constant ϑ to those based on erroneous values of these model parameters for operation point a of the boiling curve of Fig. 6. The differences in the surface heat flux and temperature estimates are plotted over time. The amplitude errors of the estimated heat flux are considerably smaller due to errors for uncertainties in the thermocouple position (Fig. 9) than for those due to its time constant (Fig. 10), if the assumed relative parameter errors are taken into account. In both cases no mean offset in the heat flux estimate occurs, since both parameters only affect the dynamics of the process. They are meaningless for the steady-state (or mean) values. A higher (lower) value of the time constant or radial position reflects a higher (lower) value of the time lag between measured temperature and surface temperature. This difference in the mod-

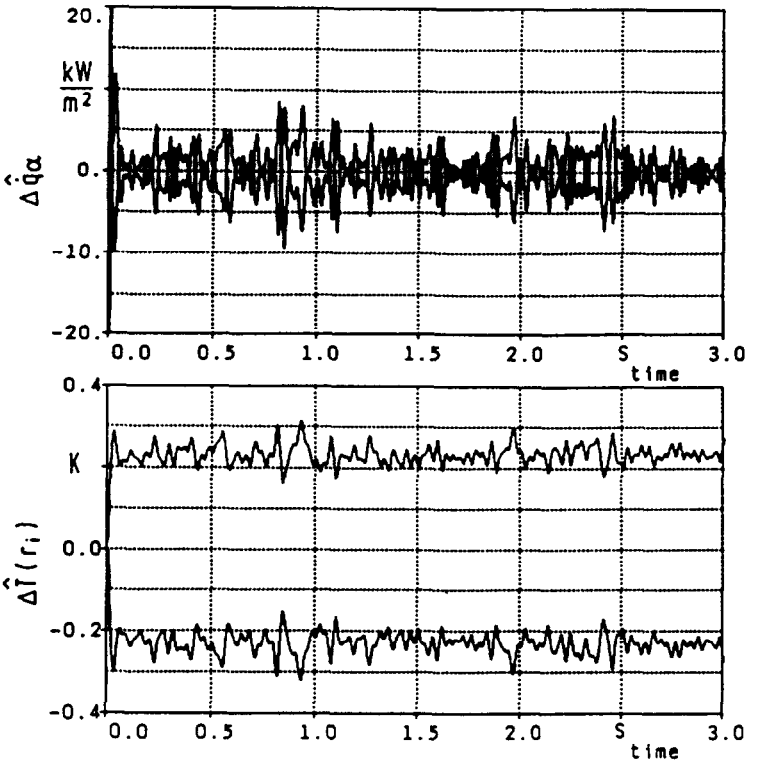

FIG. 9. Sensitivity of the estimation to errors in r_M, $r_{M,nom} = 0.25$ mm; assumed parameter error ± 0.05 mm.

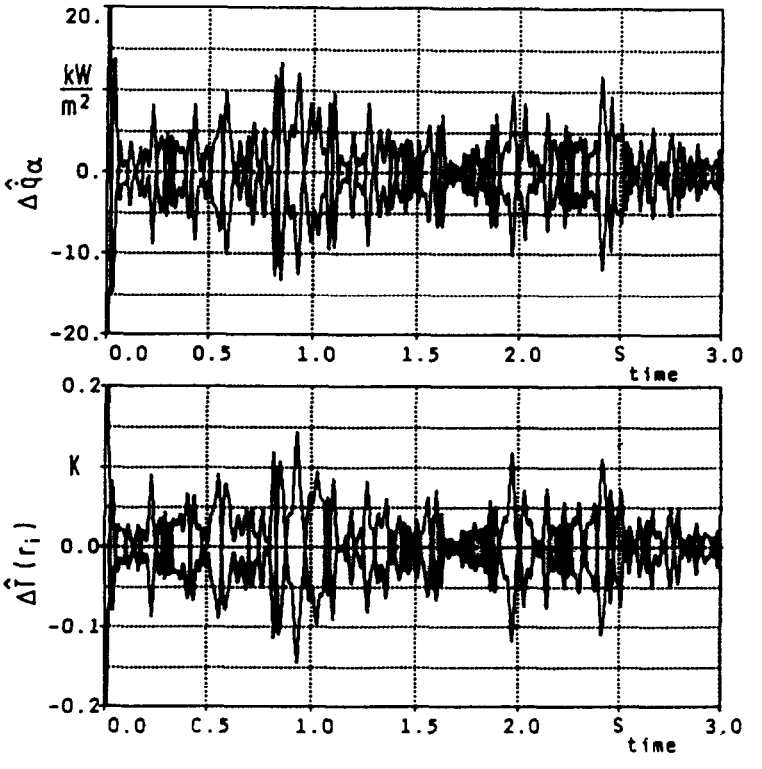

FIG. 10. Sensitivity of the estimation to errors in ϑ, $\vartheta_{nom} = 0.06$ s: assumed parameter error ± 0.01 s.

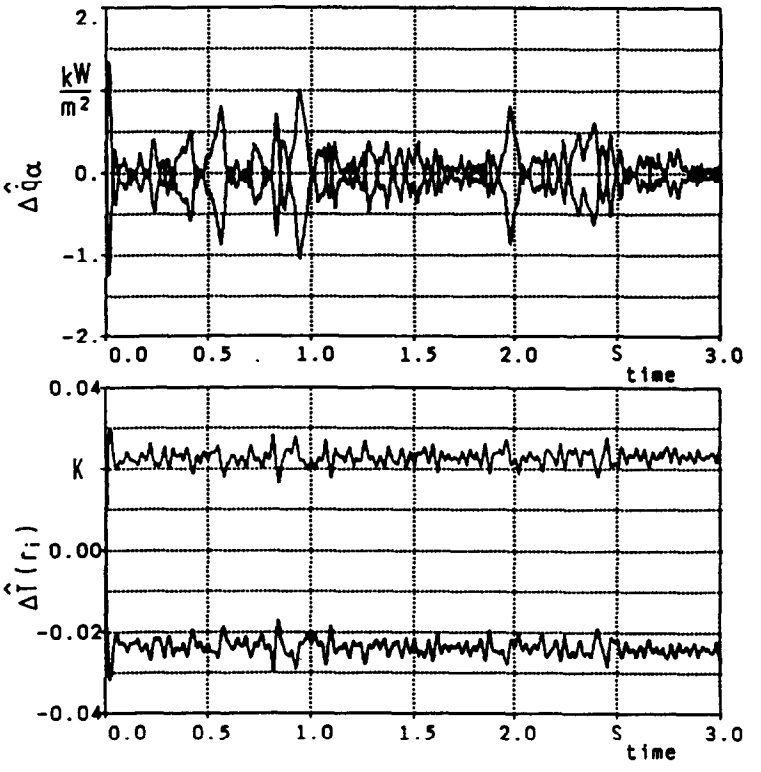

FIG. 11. Sensitivity of the estimation to errors in $\lambda^{(i)}$, $i = 1(1)3$, assumed parameter error $\pm 2\%$.

elled time lag leads to an underestimation (overestimation) of the surface heat flux peaks. If these errors occurred in the real experiment, they cannot be neglected because of the significant amplitude errors (Figs. 9 and 10). However, we feel that the experimentally determined [23, 25] nominal parameter values used in the computations are the best to describe our setup. Figure 11 shows the sensitivity of the estimation results with respect to thermal conductivity errors. The estimated surface temperature and heat flux are higher (lower) in the mean for a higher (lower) conductivity. However, the effects are negligibly small even for errors of a few percent in the thermal conductivity.

To check the sensitivity of the estimation results with respect to differing disturbance models an alternative description has been compared to the simple model of this study in ref. [25]. It assumes a proportionality between heat flux and temperature difference between fluid and evaporator wall. The heat transfer coefficient has been estimated in this case. The mean surface heat flux is slightly lower with the latter model whereas the signal characteristics and amplitudes are retained.

The last modelling error to be discussed here is related to the structure of the evaporator model which is only one-dimensional in the radial direction. To simplify the analysis heat fluxes in the other two directions have been neglected. A simple theoretical analysis of the resulting error which is based on an energy balance of a volume element containing the thermocouple dip is carried out in ref. [23]. The real amplitudes are always larger than those calculated by the one-dimensional model. The deviations are, however, shown to be less than 20%.

If measurement or quantization noise (as a consequence of A/D conversion) is present high corrections (k, φ) tend to amplify the noise leading to enlarged heat flux amplitudes. The magnitude of such errors can be checked by simulation experiments, if sufficient information on the noise signal is available. The type of quantization errors can be determined rather precisely from the experimental setup. Simulations show that heat flux errors due to unavoidable quantization noise are negligibly small. A determination of the level of noise in the temperature measurements after low pass filtering is very difficult for real experimental conditions. Temperature measurements for pure convective heat transfer reveal fluctuations of a band width of 0.03 K in the low frequency range. This number could be taken as an upper limit for the level of noise. Hence, it cannot be excluded that some measurement noise superimposes the wanted signal in the frequency range below 20 Hz. Simulation experiments with a stochastic measurement error of band width 0.03 K and frequency of 15 Hz indicate an amplification of the estimated heat flux amplitudes of some 13 kW m^{-2}.

Accounting for the different sources of estimation errors it can be summarized that the signal characteristics are very close to the true ones. All signals display a phase lag of about 0.01 s. It is anticipated that the amplification of the amplitudes due to noise and their damping due to the one-dimensional calculation compensate each other to some extent. The calculated amplitudes are probably smaller than the true ones. A cautious estimate leads to a range of amplitude errors of about 10% for low frequency signals (< 10 Hz) increasing to 30% for high frequency signal components of about 20 Hz.

Since this inverse problem from transition boiling is rather difficult to solve, an alternative solution method has been applied to approve the results obtained with our method. The space marching finite difference technique of Raynaud [28] has been chosen. The sensor dynamics, which are neglected in the original algorithm, are included here by a function specification method. The tuning parameters (time and space increments) are optimized in simulations with respect to the special requirements of our problem. The estimated surface temperature and heat flux fluctuations agree very well for both methods. The signal characteristics are very similar. The signal amplitudes are slightly larger for the difference method and there is a small phase difference between the estimates of both methods as expected. This result leads us to the conclusion that either our estimation results obtained by the observer are rather reliable or that it is not possible to get any better results with other methods.

4. CONCLUSIONS

A new approach to the solution of non-linear inverse heat conduction problems by means of state and disturbance observers has been suggested. Most of Beck *et al.*'s criteria for evaluation of methods to solve inverse heat conduction problems (see p. 38 of ref. [1]) are met by this technique. The most important strengths of our approach are the insensitivity to measurement noise due to the solution of a well-posed problem (if moderate corrections are employed), the ease of implementation by modifying existing computer programs for the solution of the direct problem and the systematic treatment of the usually unknown initial temperature profile at the starting time of the algorithm. There are no restrictions with respect to the number of sensors or observations, the size of time steps or spatial intervals, the type of coordinate system or to the type of heat conducting solid. Temperature-variable properties and composite materials are permitted. The application of the method to a non-standard problem of technical significance demonstrates its flexibility. It is shown, that the dynamics of the sensor as well as additional model equations such as the control system can be incorporated straightforwardly in the estimation scheme.

One shortcoming of the method is the unavoidable phase lag and its deficiency to match the signal shape exactly in case of fast dynamics. This disadvantage can be diminished by choosing correction terms with a larger magnitude. Due to the increasing sensitivity to noise with an increasing magnitude of the corrections, a trade-off between the accuracy of the estimates and the amplification of measurement noise must be accomplished.

An alternative estimation scheme which is comparable to the observer of our investigations is a Kalman filter [29, 30]. Its structure is identical to that of the state and disturbance observer of Fig. 3. The only difference between both approaches is the way to determine the corrections k_i. While observers are designed on a pure deterministic basis by a study of stability and rate of convergence of the adjacent error equations, the Kalman filter corrections are computed to minimize the variance of the stochastic estimation errors. A further improvement of the estimation quality in case of off-line estimation can be accomplished, if an optimal smoothing filter [29] is applied. The estimate given by the smoothing filter consists of a weighted average of the estimates of two Kalman filters—a forward and a backward filter. The forward filter starts at the beginning of the measurement time series and processes only past measurements whereas the backward filter starts at its end and hence processes only future measurements. This scheme incorporates both past and future measurements to compute an actual estimate, which has been noted before [1, 7] to be advantageous with parameter estimation or difference methods. Such a smoothing filter would improve the estimation quality significantly at the expense of a more complex algorithm.

REFERENCES

1. J. V. Beck, B. Blackwell and C. R. St. Clair, *Inverse Heat Conduction. Ill-posed Problems*. Wiley, New York (1985).
2. A. N. Tikhonov and V. Y. Arsenin, *Solution of Ill-posed Problems*. Winston, Washington, DC (1977).
3. M. M. Lavrent'ev, V. G. Romanov and S. P. Shishatskii, Ill-posed problems of mathematical physics and analysis. In *Translations of Mathematical Monographs*, Vol. 64. American Mathematical Society, Providence, Rhode Island (1986).
4. J. Baumeister, *Stable Solution of Inverse Problems*. Friedr. Vieweg & Sohn, Braunschweig (1987).
5. Y. V. Kudryavtsev, *Unsteady State Heat Transfer*. Iliffe, London (1966). Translation of the Russian edition published by Izd. Akad. Nauk., Moscow (1961).
6. P. Deuflhard and E. Hairer (Editors), *Numerical Treatment of Inverse Problems in Differential and Integral Equations*. Birkhäuser, Boston (1983).
7. E. Hensel and R. G. Hills, An initial value approach to the inverse heat conduction problem. *Trans. ASME, J. Heat Transfer* **108**, 248–256 (1986).
8. M. El Bagdouri and Y. Jarny, Optimal boundary control of a thermal system. Inverse conduction problems. *Prepr. 4th IFAC Symp. "Control of Distributed Parameter Systems"*, Los Angeles, California, 30 June–2 July (1986).
9. C. F. Weber, Analysis and solution of the ill-posed inverse heat conduction problem. *Int. J. Heat Mass Transfer* **24**, 1783–1792 (1981).

10. D. Luenberger, An introduction to observers, *IEEE Trans. Aut. Control* **16**, 596–602 (1971).
11. J. O'Reilly, Observers for linear systems. In *Mathematics in Science and Engineering*, Vol. 170. Academic Press, New York (1983).
12. M. Zeitz, *Nichtlineare Beobachter für chemische Reaktoren*, VDI-Fortschr.-Ber., Reihe 8, Nr. 27. VDI-Verlag, Düsseldorf (1977).
13. M. Köhne, *Zustandsbeobachter für Systeme mit verteilten Parametern—Theorie und Anwendung*, VDI-Fortschr.-Ber., Reihe 8, Nr. 26. VDI-Verlag, Düsseldorf (1977).
14. E. D. Gilles, Some new approaches for controlling complex processes in chemical engineering. *Proc. Chem. Process Control—CPC III*, pp. 689–747. Elsevier, New York (1986).
15. G. Juen und M. Zeitz, Beobachter im praktischen Einsatz. In *Fachberichte Messen, Steuern, Regeln*, Band 10, *Forschritte durch die digitale Meß- und Automatisierungstechnik* (Edited by M. Syrbe and M. Thoma), pp. 240–259. Springer, Berlin (1983).
16. P. Hippe and Ch. Wurmthaler, *Zustandsregelung*. Springer, Berlin (1985).
17. P. V. Tsoi, A method for calculating direct and inverse problems of unsteady-state heat transfer, *Int. J. Heat Mass Transfer* **31**, 497–504 (1988).
18. E. D. Gilles, *Systeme mit verteilten Parametern*. Oldenbourg, München (1973).
19. W. Schmid and M. Zeitz, Grenzübergang Beobachter—Differenzierer, *Regelungstechnik* **29**, 270–274 (1981).
20. M. Zeitz, Transfer characteristics of extremely fast state feedback and observer systems, *Int. J. Syst. Sci.* **14**, 169–177 (1983).
21. M. B. Carver, Method of lines solution of differential equations. In *Foundations of Computer-aided Chemical Process Design* (Edited by R. S. H. Mah and W. Seider), Vol. I, pp. 369–402. Engineering Foundation, New York (1981).
22. G. D. Byrne and A. C. Hindmarsh, Stiff ODE's solvers: a review of current and coming attractions, *J. Comp. Phys.* **70**, 1–62 (1987).
23. H. Auracher, *Partielles Filmsieden in Zweiphasenströmungen*, VDI-Fortschr.-Ber., Reihe 3, Nr. 142. VDI-Verlag, Düsseldorf (1987).
24. H. Auracher and W. Marquardt, The dither-technique for steady-state transition boiling measurements, *Proc. 8th Int. Heat Transfer Conf.*, San Francisco, California, 17–22 August, Vol. 2, pp. 501–506 (1986).
25. W. Marquardt and H. Auracher, An observer-based solution of an inverse heat transfer problem in transition boiling, *Proc. 5th IFAC Symp. "Control of Distributed Parameter Systems"*, Perpignan, France, 26–29 June, pp. 221–226 (1989).
26. W. Marquardt, P. Holl, D. Butz and E. D. Gilles, DIVA—a powerful tool for dynamic process simulation, *Chem. Engng Technol.* **10**, 164–173 (1987).
27. W. Marquardt, M. Wurst, P. Holl and E. D. Gilles, Tools of dynamic process simulation and its application. In *DECHEMA Monographs*, Vol. 115, *Modern Computer Technologies and their Effects on Chemical Technology* (Edited by R. Eckermann), pp. 485–492. VCH Verlagsgesellschaft, Weinheim (1989).
28. M. Raynaud, Détermination du flux surfacique traversant une paroi a partir de mésures de temperatures internes, Ph.D. Thesis, Université Pierre et Marie Curie, Paris, France (1984).
29. A. Gelb (Editor), *Applied Optimal Estimation*. MIT Press, Cambridge, Massachusetts (1974).
30. W. H. Ray and D. G. Lainiotis (Editors), *Distributed Parameter systems: Identification, Estimation and Control*. Marcel Dekker, New York (1978).
31. W. Walter, *Gewöhnliche Differentialgleichungen*, Zweite Auflage. Springer, Berlin (1976).
32. R. Courant and D. Hilbert, *Methoden der Mathematischen Physik I*, Dritte Auflage. Springer, Berlin (1968).

APPENDIX A. DEVELOPMENT OF THE CHARACTERISTIC EQUATION (30)

The development of the characteristic equation (30) requires the statement of the eigenvalue problem of the error equations (25)–(29). The errors may be expressed by the infinite Fourier series

$$e(z,t) = \sum_{i=1}^{\infty} \psi_i(z)\, e^{s_i t}, \quad \varepsilon(t) = \sum_{i=1}^{\infty} \alpha_i\, e^{s_i t}$$

which converge uniformly in z and t. These trial functions are introduced in the homogeneous error equations (25)–(29). Each of the resulting four equations consists of an infinite series which is equated to zero. The equations are fulfilled if each of the terms in the series is equated to zero. The following eigenvalue problem of Sturm–Liouville type results after elimination of the Fourier coefficients α_i if the index i is omitted

$$a\frac{d^2\psi}{dz^2}(z) = (s+\varphi)\psi(z)$$

$$\frac{d\psi}{dz}(0) - \frac{k}{s}\psi(\xi) = 0, \quad \frac{d\psi}{dz}(1) = 0.$$

The trial function

$$\psi(z) = A\sinh \gamma z + B\cosh \gamma z$$

equates the differential equation to zero for arbitrary constants of integration A and B. If the trial function is inserted in the homogeneous boundary conditions of the eigenvalue problem the characteristic equation (30) results after some algebraic manipulations.

It should be noted, that this approach requires an expansion theorem which guarantees the expandability of an arbitrary function by an infinite series of eigenfunctions $\psi(z)$ in $(0, 1)$. A proof of such a theorem is standard for the eigenvalue problem above if $k = 0$ (see for example p. 185 of ref. [31] or Chap. V of ref. [32]). A proof for $k \neq 0$ is not yet known.

APPENDIX B. SOME LIMITING CASES FOR THE ASYMPTOTIC ESTIMATION ERROR $\bar{\varepsilon}(t)$ OF EQUATION (38)

The limiting cases discussed in this appendix are the basis of the guide lines in Section 2.2. Note that

$$\rho = \sqrt{\left(\frac{\varphi}{a}\right)}$$

is a large number even for moderate values of φ. For metals, a heat conducting body of length $L = 1$ m and a reference time of 1 s dimensionless a is of magnitude 10^{-4}. The number κ used in the approximations below is from $(0, 1)$.

For small coordinates ξ

$$\bar{\varepsilon}(t)_{\xi\to 0} = \frac{\rho^2}{\cosh\rho}\int_0^1 \mu(\zeta,t)\cosh\rho(1-\zeta)\,d\zeta - \rho\tanh\rho\,\delta(t).$$

For small coordinates ξ and large tuning parameters ρ

$$\begin{aligned}\bar{\varepsilon}(t)_{\xi\to 0,\rho\to\infty} &= 2\rho^2 e^{-\rho}\int_0^1 \mu(\zeta,t)\cosh\rho(1-\zeta)\,d\zeta - \rho\,\delta(t)\\ &\approx 2\rho^2 e^{-\rho}\cosh\kappa\rho\int_0^1 \mu(\zeta,t)\,d\zeta - \rho\,\delta(t)\\ &= \rho^2(e^{\rho(\kappa-1)} + e^{-\rho(\kappa+1)})\int_0^1 \mu(\zeta,t)\,d\zeta - \rho\,\delta(t)\\ &\to -\rho\,\delta(t).\end{aligned}$$

For large coordinates ξ

$$\tilde{\varepsilon}(t)_{\xi \to 1} \approx \rho^2 \cosh \kappa\rho \int_0^1 \mu(\zeta, t)\, d\zeta - \rho \sinh \rho\, \delta(t).$$

For large coordinates ξ and large tuning parameters ρ

$$\tilde{\varepsilon}(t)_{\xi \to 1, \rho \to \infty} \approx \frac{\rho^2}{2} e^{\kappa\rho} \int_0^1 \mu(\zeta, t)\, d\zeta - \frac{\rho}{2} e^{\rho}\, \delta(t).$$

UNE SOLUTION DES PROBLEMES INVERSES DE CONDUCTION THERMIQUE BASEE SUR OBSERVATEUR

Résumé—Le problème inverse de conduction thermique apparaît lorsque les températures sont mesurées à l'intérieur d'un corps pour connaître la température et le flux à la surface. On introduit une nouvelle approche pour résoudre ce problème. Elle repose sur le concept des observateurs d'état et de perturbation bien connu dans la théorie des systèmes. Le profil complet de température dans le corps aussi bien que la température et le flux à la surface peuvent être calculés à partir d'une ou plusieurs mesures de température à l'intérieur, à l'aide d'un observateur paramétrique distribué non linéaire. La technique est introduite et analysée théoriquement sur un exemple simple. L'approche est finalement appliquée à un problème difficile et significatif en pratique. On évalue l'évolution des oscillations locales du flux thermique et de la température sur la face interne d'un tube évaporateur pendant des conditions transitoires d'ébullition. On présente des résultats expérimentaux d'ébullition pour un réfrigérant R114 s'écoulant en ascension dans un tube chauffé électriquement.

DIE LÖSUNG INVERSER WÄRMELEITPROBLEME MIT HILFE VON BEOBACHTERN

Zusammenfassung—Ein inverses Wärmeleitproblem liegt dann vor, wenn die Temperatur im Inneren eines Körpers gemessen wird und daraus die Temperatur und der Wärmestrom an der Oberfläche ermittelt werden soll. Es wird eine neuartige Methode zur Lösung derartiger Probleme vorgestellt. Sie beruht auf dem Konzept der Zustands- und Störgrößenbeobachter, das in der Systemtheorie wohlbekannt ist. Aus einer oder mehreren Temperaturmessungen im Inneren können mittels eines nichtlinearen Beobachters für Systeme mit verteilten Parametern das Temperaturprofil im wärmeleitenden Körper einschließlich der Temperatur und des Wärmestroms an der Oberfläche bestimmt werden. Die Rechentechnik wird zunächst anhand eines einfachen Beispiels eingeführt und analysiert. Sodann wird das Verfahren auf ein schwieriges technisch relevantes Problem angewandt: Es wird die zeitliche Änderung lokaler Werte der Wärmestromdichte und der Temperatur an der inneren Oberfläche eines Verdampferrohres im Bereich des Übergangssiedens ermittelt. Als Grundlage dienen Messungen mit Kältemittel 114 bei Aufwärtsströmung im senkrechten elektrisch beheizten Rohr.

РЕШЕНИЕ ОБРАТНЫХ ЗАДАЧ ТЕПЛОПРОВОДНОСТИ, ОСНОВАННОЕ НА ПРИНЦИПЕ НАБЛЮДАЕМОСТИ

Аннотация—Обратная задача теплопроводности состоит в определении температуры и теплового потока на поверхности тела из измерений температуры в теле. Описывается новый подход к решению данного класса задач, основанный на понятии наблюдаемости состояния и возмущения, известном из теории систем. Полный температурный профиль в теле, а также тепловой поток и температура на поверхности могут быть рассчитаны по одному или нескольким измерениям внутренней температуры при помощи принципа наблюдаемости нелинейного распределенного параметра. Данный метод теоретически анализируется на простом примере. Затем он применяется к сложной обратной задаче, важной в техническом отношении. Оценивается развитие во времени колебаний локальных тепловых потоков и температур на внутренней поверхности трубки испарителя в условиях переходного режима кипения. Представлены экспериментальные данные для восходящего течения кипящего хладагента R114 в трубе, нагреваемой электрическим током.